

# Complex dynamics in hard oscillators: the influence of constant inputs

V. Lanza<sup>a,\*</sup>, L. Ponta<sup>b</sup>, M. Bonnin<sup>a</sup>, F. Corinto<sup>a</sup>

<sup>a</sup>*Department of Electronics, Politecnico di Torino, Italy*

<sup>b</sup>*Department of Physics, Politecnico di Torino, Italy*

---

## Abstract

Systems with the coexistence of different stable attractors are widely exploited in systems biology in order to suitably model the differentiating processes arising in living cells. In order to describe genetic regulatory networks several deterministic models based on systems of nonlinear ordinary differential equations have been proposed.

Few studies have been developed to characterize how either an external input or the coupling can drive systems with different coexisting states. For the sake of simplicity, in this manuscript we focus on systems belonging to the class of radial isochron clocks that exhibits hard excitation, in order to investigate their complex dynamics, local and global bifurcations arising in presence of constant external inputs. In particular the occurrence of saddle node on limit cycle bifurcations is detected.

*Keywords:* complex dynamics, bioinspired systems, hard excitation, saddle node on limit cycle bifurcation, constant input

---

## 1. Introduction

Being the most diffuse formalism to model dynamical systems in science and engineering, ordinary differential equations (ODEs) have been widely used in systems biology as well. In particular, nonlinear dynamical systems that can exhibit

---

\*Corresponding author

*Email addresses:* valentina.lanza@polito.it (V. Lanza), linda.ponta@polito.it (L. Ponta), michele.bonnin@polito.it (M. Bonnin), fernando.corinto@polito.it (F. Corinto)

coexisting stable attractors are considered of universal importance, since they allow physiologists to accurately model cell differentiation processes. One of the most interesting cases, that goes by the name of hard excitation, is the concurrence between oscillatory and non-oscillatory states (Liu, 2002; Jovanic et al., 2008; Minorsky, 1974).

It is well known the external environment (such as light and temperature) or the substrate synthesis/injection rate play an important role in the dynamics of molecular reactions (Bastin & Dochain, 1990). In order to properly model these effects, external forcing terms have to be taken into account in the mathematical modeling (Leloup & Goldbeter, 2001). Moreover, the processes inside the cell are localized in different spatial domains, while exchanges of chemical species take place in the common extracellular medium. Therefore, it is more appropriate to consider reaction diffusion or multi-compartmental equations (Jovanic et al., 2008). Actually, few studies (Goldbeter et al., 2001; Goldbeter & Berridge, 1997) have been developed to characterize how an external input or coupling effects can drive systems with different coexisting states.

Typical systems that exhibit such a dynamical behavior are represented by the so-called Cyclic Negative Feedback Systems, that arise in a variety of mathematical bio-inspired models, from cellular signal pathways (Kholodenko, 2000; Liu, 2002) to gene regulatory networks (Tyson & Othmer, 1978; de Jong, 2002; Elowitz & Leibler, 2000). Cyclic Negative Feedback systems (CNF systems) are described by the following set of nonlinear differential equations (Arcak & Sontag, 2008):

$$\begin{cases} \dot{x}_1 = -g_1(x_1) + f_n(x_n) \\ \dot{x}_k = -g_k(x_k) + f_{k-1}(x_{k-1}), & 2 \leq k \leq n \end{cases}$$

where  $x_k$  only assumes positive values,  $g_p(\cdot)$  ( $p = 1, \dots, n$ ) and  $f_q(\cdot)$  ( $q = 1, \dots, n-1$ ) are increasing functions, while  $f_n(\cdot)$  is a decreasing function. The first-order time derivative of  $x_k$  is denoted by  $\dot{x}_k$ . The variables  $x_k$  can represent the concentrations of certain molecules (e.g. mRNA, proteins) in the cell. In addition, the function  $f_n(\cdot)$  suitably reproduces the inhibition of  $x_1$  by the chemical product  $x_n$ . It is easy to deduce from the previous expression that each variable  $x_k(t)$  is activated by its previous neighbor  $x_{k-1}(t)$ , except for  $x_1(t)$  that is repressed by  $x_n(t)$ . It can be proved (Arcak & Sontag, 2008) that CNF systems exhibit a global asymptotic stable equilibrium  $\mathbf{x}^* = (x_1^*, \dots, x_n^*)$ , provided the secant criterion (Thron, 1991) is satisfied. Furthermore, for these type of systems the Poincaré-Bendixson Theorem holds (Mallet-Paret & Smith, 1990), that is the coexistence between stable equilibria and periodic orbits is allowed.

In (Lanza et al., 2009), we have analyzed the effect of coupling on arrays of diffusively coupled third order CNF systems. We have shown that CNF arrays with diffusive couplings that are constant and local (i.e. they involve only the two nearest neighbors of each CNF system) are potentially equivalent to nonlinear networks whose elements are fully connected (i.e. each subsystem is linked to all the others). Moreover, we have shown that already in a two-compartment version of CNF systems new dynamics, such as global periodic oscillations with space-variant amplitude (e.g., discrete breathers-like patterns), can arise due to the couplings.

One of the main drawbacks of CNF systems is that they can be of high order and quite difficult to handle. Even for the network of third order systems analyzed in (Lanza et al., 2009), it is mathematically complicated to detect and characterize all the new periodic solutions to whom the coupling or an external input give rise. Therefore, in order to investigate the emergence of such new dynamics, we consider a nonlinear dynamical system that is easier to handle and that for certain values of its parameters has qualitatively the same dynamical behavior of a CNF system. First of all, we focus on the single system and carry out a complete analysis of both the local and global bifurcations arising in presence of constant external inputs. In particular, we show the occurrence of saddle node on limit cycle bifurcations and that in presence of such bifurcations our system behaves as a relaxation oscillator.

This manuscript is structured as follows. In Section 2 we introduce the model under study, i.e. a radial isochron clock with hard excitation that is well known in literature as the normal form for the Bautin bifurcation (Kuznetsov, 2004; Izhikevich, 2001). Moreover, we investigate how this system changes its form due to the presence of a constant external input. In Section 3 a complete analysis of local and global bifurcations arising in presence of constant external inputs is carried out. In particular, we show that the periodic solutions of our system can disappear through saddle node on limit cycle bifurcations. Section 4 is devoted to conclusions.

## 2. The case of radial isochron clocks

Let us consider a simpler model with respect to CNF systems but with the same dynamics:

$$\dot{z} = (\sigma_0 + j\Omega_0)z + \sigma_1|z|z + \sigma_2|z|^2z + I_0, \quad (1)$$

where  $z = re^{j\phi} \in \mathbf{C}$  is a complex variable,  $\Omega_0 > 0$  and  $\sigma_0, \sigma_1, \sigma_2$  are real parameters. The term  $I_0$  represents the action of a constant external input and from now on we will assume  $I_0 > 0$  without any loss of generality<sup>1</sup>.

*Absence of constant external input*

In the  $(r, \phi)$  coordinates, system (1) with  $I_0 = 0$  can be recast as:

$$\begin{cases} \dot{r} = r(\sigma_0 + \sigma_1 r + \sigma_2 r^2) \\ \dot{\phi} = \Omega_0. \end{cases} \quad (2)$$

It is worth noting that (2) belongs to the category of the radial isochron clocks proposed by Winfree (Winfree, 2001), and it has been widely exploited as a simplified model for the Hodgkin-Huxley neuron (Boushel & Curran, 2007) and for studying the phenomenon of cardiac fibrillation (de Paor, 1994).

This system can be easily investigated since the study of the periodic solutions of (2) reduces to the analysis of the equilibria of the first equation of (2). It is easy to see that

- a Hopf bifurcation takes place for  $\sigma_0 = 0$ , which is subcritical for  $\sigma_1 > 0$  and supercritical otherwise;
- a double limit cycle bifurcation (also known as fold, or tangent, or saddle-node bifurcation of limit cycles) occurs for  $\sigma_1^2 - 4\sigma_0\sigma_2 = 0$ , and  $\sigma_1 \geq 0$ . A double limit cycle bifurcation occurs when a branch of stable periodic solutions and a branch of unstable periodic solutions coalesce and obliterate each other at the bifurcation point (Guckenheimer & Holmes, 1983; Kuznetsov, 2004);
- this system can undergo a Bautin bifurcation, when a Hopf bifurcation and a double limit cycle bifurcation occur simultaneously (Kuznetsov, 2004; Izhikevich, 2001). In our case it happens for  $\sigma_0 = \sigma_1 = 0$  but  $\sigma_2 \neq 0$ . When  $\sigma_2 < 0$ , the Bautin bifurcation is said to be supercritical, while for  $\sigma_2 > 0$  it is subcritical. In particular, for  $\sigma_2 < 0$  the cycle with larger amplitude is stable.

The complete bifurcation diagram is represented in Figure 1.

---

<sup>1</sup>It is easy to notice that the system is invariant under the transformation  $z \rightarrow -z, I_0 \rightarrow -I_0$ .

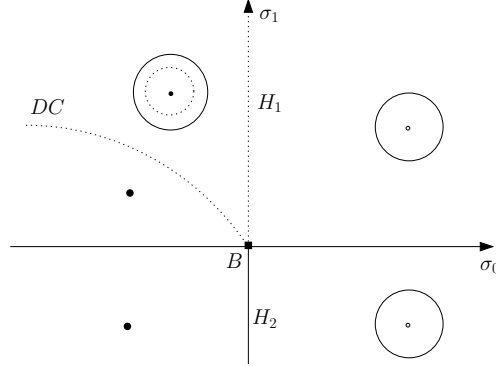


Figure 1: Bifurcation diagram for the single radial isochron clock (2). The different bifurcation curves are labeled as follows:  $H_1$  stands for subcritical Hopf bifurcation,  $H_2$  for supercritical Hopf bifurcation,  $DC$  for double limit cycle bifurcation, and  $B$  for Bautin bifurcation. The dotted line where a  $DC$  bifurcation occurs has equation  $\sigma_1^2 - \sigma_0\sigma_2 = 0$ .

In the following, we are interested in studying a system that presents a hard excitation behavior, thus we focus on a choice of the parameters such that we have the coexistence of a stable equilibrium point and a stable limit cycle:

$$\begin{cases} \sigma_1^2 - 4\sigma_0\sigma_2 > 0 \\ \sigma_1 > 0 \\ \sigma_2 < 0. \end{cases} \quad (3)$$

In Figure 2 the phase portrait of our system is represented. We have a sort of concentric structure of cycles, where the origin is a stable equilibrium point, surrounded by two closed curves alternatively stable and unstable. Thus, it is easy to understand why a similar configuration goes by the name of hard excitation (Minorsky, 1974): if the systems is in the steady state, then it needs a strong perturbation to cross the separatrix and start to oscillate.

#### *Presence of external constant input*

In order to simplify the notation and reduce the number of control parameters, we rescale the variables involved in (1) in the following way:

$$(z, t) \rightarrow \left( \sqrt{\frac{|\sigma_0|}{|\sigma_2|}} z, \frac{t}{|\sigma_0|} \right).$$

Thus, from (1) we obtain the system

$$\dot{z} = (\text{sgn } \sigma_0 + j\Omega)z + \alpha|z|z + \text{sgn } \sigma_2|z|^2z + I, \quad (4)$$

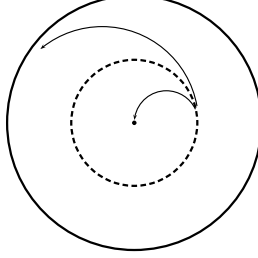


Figure 2: Phase portrait of a system with hard excitation. The stable equilibrium point and the stable limit cycle (solid line) are separated by an unstable limit cycle (dashed line).

where  $\text{sgn}(\cdot)$  is the sign function and

$$\Omega = \frac{\Omega_0}{|\sigma_0|} \quad \alpha = \frac{\sigma_1}{\sqrt{|\sigma_0 \sigma_2|}} \quad I = \sqrt{\left| \frac{\sigma_2}{\sigma_0} \right|} \frac{I_0}{|\sigma_0|}. \quad (5)$$

Conditions (3) imply  $\text{sgn} \sigma_0 = -1$ ,  $\text{sgn} \sigma_2 = -1$ ,  $\alpha > 2$ , and thus system (4) becomes

$$\dot{z} = (-1 + j\Omega)z + \alpha|z|z - |z|^2z + I. \quad (6)$$

Exploiting the cartesian coordinates ( $z = x + jy$ ), system (6) can be rewritten as

$$\begin{cases} \dot{x} = (-1 + \alpha\sqrt{x^2 + y^2} - (x^2 + y^2))x - \Omega y + I \\ \dot{y} = (-1 + \alpha\sqrt{x^2 + y^2} - (x^2 + y^2))y + \Omega x, \end{cases} \quad (7)$$

or to simplify notation

$$\begin{cases} \dot{x} = g(x, y)x - \Omega y + I \\ \dot{y} = g(x, y)y + \Omega x, \end{cases} \quad (8)$$

where  $g(x, y) = (-1 + \alpha\sqrt{x^2 + y^2} - (x^2 + y^2))$ .

First of all, in order to characterize the dynamics of this system, we are interested in finding all the equilibrium configurations. Thus, we have to solve the following set of nonlinear algebraic equations:

$$\begin{cases} g(x, y)x - \Omega y + I = 0 \\ g(x, y)y + \Omega x = 0. \end{cases} \quad (9)$$

From the second equation we obtain

$$g(x,y) = -\Omega \frac{x}{y}, \quad (10)$$

having assumed<sup>2</sup>  $y \neq 0$ . The substitution of expression (10) in the first equation of (9) yields

$$-\Omega \frac{x^2}{y} - \Omega y + I = 0. \quad (11)$$

The solutions of (8) are precisely the intersection points between the circumference  $\Gamma : x^2 + (y - \frac{I}{2\Omega})^2 = (\frac{I}{2\Omega})^2$  and the curve  $S : x = -\frac{1}{\Omega}yg(x,y)$ . Moreover, from (11) we can conclude that all the equilibrium configurations have a positive  $y$ -component. Furthermore, since from (11) we have  $x^2 + y^2 = \frac{I}{\Omega}y$ , we can notice that actually  $S$  has the following expression:

$$S : x = -\frac{1}{\Omega} \left[ -1 + \alpha \sqrt{\frac{I}{\Omega}y - \frac{I}{\Omega}y} \right],$$

and we can derive that the equilibrium points of system (8) are the intersections between the curves:

$$\begin{cases} \Gamma : x^2 + (y - \frac{I}{2\Omega})^2 = (\frac{I}{2\Omega})^2 \\ S : x = -\frac{1}{\Omega} \left[ -1 + \alpha \sqrt{\frac{I}{\Omega}y - \frac{I}{\Omega}y} \right]. \end{cases} \quad (12)$$

Substituting the second equation of (12) in the first one, and introducing the new variable  $\zeta = \sqrt{\frac{I}{\Omega}y}$ , we finally conclude that the equilibrium points of system (7) are the roots of the following polynomial:

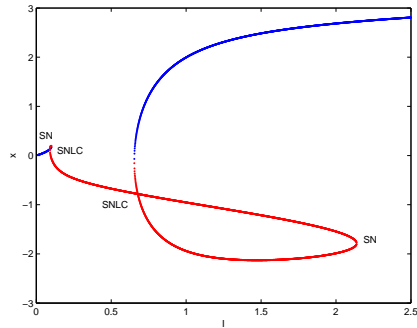
$$\zeta^6 - 2\alpha\zeta^5 + (\alpha^2 + 2)\zeta^4 - 2\alpha\zeta^3 + (1 + \Omega^2)\zeta^2 - I^2 = 0. \quad (13)$$

It is worth noting that, due to the definition of  $\zeta$ , we are interested only in the real and positive roots of (13).

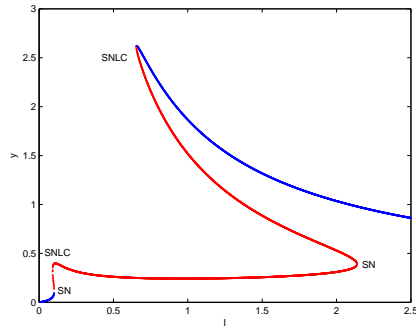
By choosing  $\alpha = 3$ , in Figure 3 the equilibrium configurations and their stability properties as function of  $I$  for different fixed values of  $\Omega$  are represented. Depending on the values of the two parameters  $\Omega$  and  $I$ , a different number of solutions and therefore different dynamical behaviors are admissible.

---

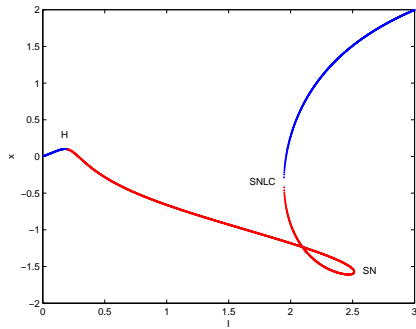
<sup>2</sup>The case  $y = 0$  can be treated separately and is not interesting for our study. In fact, from (9) we can conclude that  $y = 0$  implies  $x = 0$  and  $I = 0$ . Thus, a solution with  $y = 0$  can be achieved only in absence of external input.



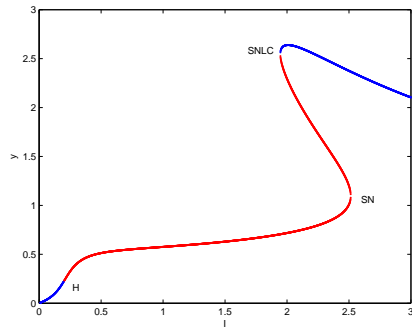
(a)



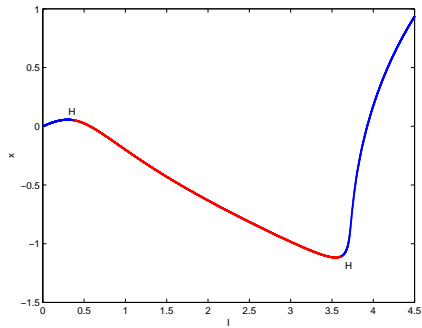
(b)



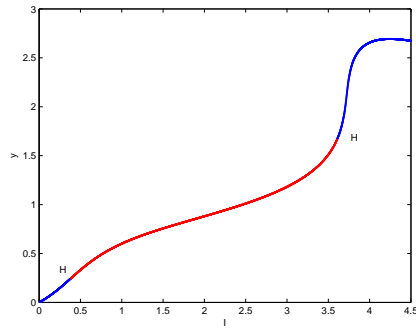
(c)



(d)



(e)



(f)

Figure 3: Stable (in blue) and unstable (in red) equilibrium configurations of system (7) as function of the parameter  $I$ , for different values of  $\Omega$  (in (a) and (b)  $\Omega = 0.25$ , in (c) and (d)  $\Omega = 0.75$ , in (e) and (f)  $\Omega = 1.5$ ). Here  $\alpha$  is set equal to 3. In the left and right columns the  $x$  and  $y$ -components are represented, respectively. The bifurcations are indicated as follows: SN= saddle-node, SNLC= saddle-node on limit cycle, H= Hopf.



### 3. Bifurcation analysis

In this section we study the bifurcations occurring in system (7) as the parameters  $(\Omega, I)$  are varied.

We have seen in the previous section that in absence of external input ( $I = 0$ ) the system presents two nested periodic solutions, one stable and one unstable, for every value of  $\Omega$ . For small values of  $I$ , these solutions are maintained, but, increasing the intensity of the input, they disappear through a sequence of different both local and global bifurcations.

#### 3.1. Local bifurcations

In order to investigate local bifurcations of equilibria in system (7) we shall look at the polynomial discriminant of (13), and at the linearization of (7) in the neighborhood of the equilibrium points. A polynomial discriminant is defined as the product of the squares of the differences of the polynomial roots  $s_i$ . For a polynomial of degree  $n$  in the form

$$q(x) = a_n x^n + a_{n-1} x^{n-1} + \dots + a_1 x + a_0 = 0$$

the discriminant is defined as (Cohen, 1993)

$$D_n = a_n^{2n-2} \prod_{\substack{i,j \\ i < j}}^n (s_i - s_j)^2. \quad (14)$$

Since the discriminant vanishes in presence of a multiple root, the values of  $\Omega$  and  $I$  for which the discriminant  $D$  is equal to zero identify loci of coalescences or births of solutions, and therefore possible bifurcations. In Figure 4 the curves  $D = 0$  for (13) in the  $\Omega - I$  plane for  $\alpha = 3$  are represented.

Now we turn our attention at the linearization of (7). The Jacobian matrix of system (6), evaluated in the equilibrium points  $(\bar{x}, \bar{y})$ , has the following expression:

$$J = \begin{pmatrix} g(\bar{x}, \bar{y}) + \bar{x}^2 h(\bar{x}, \bar{y}) & \bar{x}\bar{y}h(\bar{x}, \bar{y}) - \Omega \\ \bar{x}\bar{y}h(\bar{x}, \bar{y}) + \Omega & g(\bar{x}, \bar{y}) + \bar{y}^2 h(\bar{x}, \bar{y}) \end{pmatrix}, \quad (15)$$

where

$$h(\bar{x}, \bar{y}) = \frac{\alpha}{\sqrt{\bar{x}^2 + \bar{y}^2}} - 2. \quad (16)$$

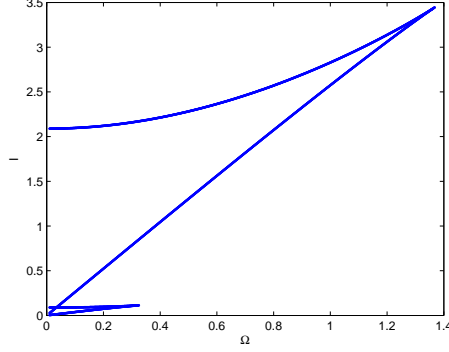


Figure 4: The locus of parameters where the discriminant of polynomial (13) with  $\alpha = 3$  annihilates. This points out the possible occurrence of bifurcations of equilibria in the system.

The sign of the real part of the eigenvalues can be determined by looking at the trace and the determinant of the Jacobian matrix. In the present case they are given by

$$\begin{aligned}
\text{tr}J &= 2g(\bar{x}, \bar{y}) + (\bar{x}^2 + \bar{y}^2)h(\bar{x}, \bar{y}) \\
&= 2(-1 + \alpha\sqrt{\bar{x}^2 + \bar{y}^2} - (x^2 + y^2)) + (\bar{x}^2 + \bar{y}^2) \left( \frac{\alpha}{\sqrt{\bar{x}^2 + \bar{y}^2}} - 2 \right) \\
&= 2(-1 + \alpha\bar{\zeta} - \bar{\zeta}^2) + \alpha\bar{\zeta} - 2\bar{\zeta}^2 \\
&= -4\bar{\zeta}^2 + 3\alpha\bar{\zeta} - 2,
\end{aligned} \tag{17}$$

$$\begin{aligned}
\det J &= (g(\bar{x}, \bar{y}) + \bar{x}^2 h(\bar{x}, \bar{y}))(g(\bar{x}, \bar{y}) + \bar{y}^2 h(\bar{x}, \bar{y})) - (\bar{x}\bar{y}h(\bar{x}, \bar{y}) - \Omega)(\bar{x}\bar{y}h(\bar{x}, \bar{y}) + \Omega) \\
&= (g(\bar{x}, \bar{y}))^2 + (\bar{x}^2 + \bar{y}^2)g(\bar{x}, \bar{y})h(\bar{x}, \bar{y}) - \Omega^2 \\
&= \frac{\Omega I}{\bar{y}} - I\bar{x}h(\bar{x}, \bar{y}) \\
&= \frac{\Omega I}{\bar{y}} + \frac{I}{\Omega}\bar{y} \left[ -1 + \alpha\sqrt{\frac{I}{\Omega}\bar{y}} - \frac{I}{\Omega}\bar{y} \right] \left( \frac{\alpha}{\sqrt{\frac{I}{\Omega}\bar{y}}} - 2 \right) \\
&= \frac{I^2}{\bar{\zeta}^2} + \bar{\zeta} \left[ -1 + \alpha\bar{\zeta} - \bar{\zeta}^2 \right] (\alpha - 2\bar{\zeta}),
\end{aligned} \tag{18}$$

having exploited relations (10), (12), and (16), and having introduced the ancillar

variable  $\bar{\zeta} = \sqrt{\frac{I}{\Omega}\bar{y}}$ .

Time-domain simulations show that for certain values of  $\Omega$  and  $I$  system (7) exhibits Hopf bifurcations. The conditions for the occurrence of this bifurcation are the following (Kuznetsov, 2004):

$$\begin{cases} \text{tr}J = 0 \\ \det J > 0. \end{cases} \quad (19)$$

From (17), condition  $\text{tr}J = 0$  leads to

$$-4\bar{\zeta}^2 + 3\alpha\bar{\zeta} - 2 = 0, \quad (20)$$

that is

$$\bar{\zeta}_{1,2} = \frac{3\alpha \pm \sqrt{9\alpha^2 - 32}}{8}. \quad (21)$$

These two solutions exist only for  $9\alpha^2 - 32 \geq 0$ , that is only for  $\alpha \geq \frac{4\sqrt{2}}{3} \cong 1.886$ . However, this condition is always satisfied, since  $\alpha > 2$  due to (3).

From the definition of  $\bar{\zeta}$  and from (12), we can find the coordinates of the equilibrium points  $P_1 = (\bar{x}_1, \bar{y}_1)$  and  $P_2 = (\bar{x}_2, \bar{y}_2)$ , at which the trace of the Jacobian annihilates:

$$\begin{aligned} \bar{y}_i &= \frac{\Omega}{I}\bar{\zeta}_i^2 \\ \bar{x}_i &= -\frac{1}{\Omega} \left[ -1 + \alpha\bar{\zeta}_i - \bar{\zeta}_i^2 \right] \quad i = 1, 2. \end{aligned}$$

Substituting (21) into (13) we obtain the Hopf bifurcation curves in the parameters plane

$$I^2 = I_i^2 = \bar{\zeta}_i^6 - 2\alpha\bar{\zeta}_i^5 + (\alpha^2 + 2)\bar{\zeta}_i^4 - 2\alpha\bar{\zeta}_i^3 + (1 + \Omega^2)\bar{\zeta}_i^2 \quad i = 1, 2. \quad (22)$$

For instance, with  $\alpha = 3$  (the case considered in Figure 3) we have

$$\begin{aligned} \bar{\zeta}_1 = \frac{1}{4} &\Rightarrow P_1 = \left( -\frac{5}{16\Omega}, \frac{\Omega}{16I_1} \right) \\ I_1^2 &= \frac{25 + 256\Omega^2}{4096} \\ \bar{\zeta}_2 = 2 &\Rightarrow P_2 = \left( -\frac{1}{\Omega}, \frac{4\Omega}{I_2} \right) \\ I_2^2 &= 4(1 + \Omega^2). \end{aligned}$$

Actually, we still have to discriminate between Hopf bifurcations and neutral saddles (Kuznetsov, 2004), exploiting the condition on the determinant of the Jacobian matrix. Introducing again the variable  $\bar{\zeta}_i = \sqrt{\frac{I_i}{\Omega} \bar{y}_i}$ , and recalling the expression for  $I_i$  in (22), we get

$$\begin{aligned} \det J|_{P_i} &= \frac{I_i^2}{\bar{\zeta}_i^2} + \bar{\zeta}_i \left[ -1 + \alpha \bar{\zeta}_i - \bar{\zeta}_i^2 \right] \left( \alpha - 2\bar{\zeta}_i \right) \\ &= \frac{\bar{\zeta}_i^6 - 2\alpha \bar{\zeta}_i^5 + (\alpha^2 + 2)\bar{\zeta}_i^4 - 2\alpha \bar{\zeta}_i^3 + (1 + \Omega^2)\bar{\zeta}_i^2}{\bar{\zeta}_i^2} + \bar{\zeta}_i \left[ -1 + \alpha \bar{\zeta}_i - \bar{\zeta}_i^2 \right] \left( \alpha - 2\bar{\zeta}_i \right) \\ &= 3\bar{\zeta}_i^4 - 5\alpha \bar{\zeta}_i^3 + 2(\alpha^2 + 2)\bar{\zeta}_i^2 - 3\alpha \bar{\zeta}_i + (1 + \Omega^2). \end{aligned}$$

Requiring the positivity of  $\det J$ , it yields

$$\begin{aligned} \det J|_{P_i} > 0 \quad \Rightarrow \quad \Omega^2 > -3\bar{\zeta}_i^4 + 5\alpha \bar{\zeta}_i^3 - 2(\alpha^2 + 2)\bar{\zeta}_i^2 + 3\alpha \bar{\zeta}_i - 1 \quad (23) \\ &= \left( \frac{3}{64}\alpha^3 - \frac{1}{4}\alpha \right) \bar{\zeta}_i + \frac{1}{4} - \frac{1}{32}\alpha^2, \end{aligned}$$

where we used (20) to reduce the degree of the right hand side. In particular, substituting the values of  $\bar{\zeta}_i$  found in (21), we obtain

$$\det J|_{P_1} > 0 \quad \Rightarrow \quad \Omega^2 > \frac{9}{512}\alpha^4 + \frac{1}{4} - \frac{1}{8}\alpha^2 - \left( \frac{3}{512}\alpha^3 - \frac{1}{32}\alpha \right) \sqrt{9\alpha^2 - 32} \quad (24)$$

$$\det J|_{P_2} > 0 \quad \Rightarrow \quad \Omega^2 > \frac{9}{512}\alpha^4 + \frac{1}{4} - \frac{1}{8}\alpha^2 + \left( \frac{3}{512}\alpha^3 - \frac{1}{32}\alpha \right) \sqrt{9\alpha^2 - 32}.$$

Finally, we can conclude that for  $\alpha = 3$  in the plane  $\Omega - I$  the Hopf bifurcations occur if the following conditions are satisfied (see Figure 5):

$$\begin{cases} I^2 = \frac{25+256\Omega^2}{4096} \\ \Omega > \frac{5}{16} \end{cases} \quad \begin{cases} I^2 = 4(1 + \Omega^2) \\ \Omega > 1. \end{cases} \quad (25)$$

It is worth observing that, for the examples shown in Figure 3, we have one Hopf bifurcation for  $\Omega = 0.75$  (in this case only  $P_1$  exists) and two Hopf bifurcations for  $\Omega = 1.5$ . These situations are in perfect agreement with conditions (25).

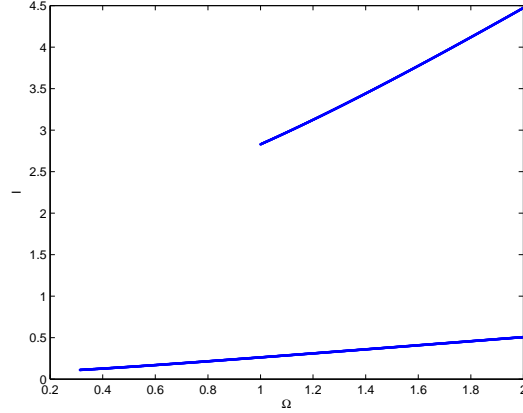


Figure 5: Curves of Hopf bifurcations in the  $\Omega - I$  plane for  $\alpha = 3$ .

**Remark 1.** *The points  $P_1$  and  $P_2$  found above have a direct relation with the curves  $\Gamma$  and  $S$  in (12). If we consider  $S$  as  $S : x = f(y)$ , then it is possible to show that  $P_1$  and  $P_2$  are the relative maximum and minimum of  $S$ , respectively. Furthermore, the values  $I_1$  and  $I_2$  are precisely the ones for which these relative maximum and minimum points lie on the circumference  $\Gamma$ .*

To determine the stability of the emerging limit cycle, we use normal form theory. We recall (Guckenheimer & Holmes, 1983) that for a planar system in the form

$$\begin{pmatrix} \dot{x} \\ \dot{y} \end{pmatrix} = \begin{pmatrix} 0 & -\omega \\ \omega & 0 \end{pmatrix} \begin{pmatrix} x \\ y \end{pmatrix} + \begin{pmatrix} F(x, y) \\ G(x, y) \end{pmatrix} \quad (26)$$

with  $F(0) = G(0) = 0$  and  $DF(0) = DG(0) = 0$ , we have to evaluate the following quantity:

$$a = \frac{1}{16} (F_{xxx} + F_{xyy} + G_{xxy} + G_{yyy}) \quad (27)$$

$$+ \frac{1}{16\omega} (F_{xy}(F_{xx} + F_{yy}) - G_{xy}(G_{xx} + G_{yy}) - F_{xx}G_{xx} + F_{yy}G_{yy}),$$

where all the partial derivatives are computed in  $(0,0)$ . Thus, if  $a < 0$  we can conclude that the Hopf bifurcation is supercritical, while if  $a > 0$  is subcritical (Guckenheimer & Holmes, 1983).

In order to proceed with the computation we have to move the bifurcation points from  $P_1$  and  $P_2$  to the origin. Let us introduce the following change of

variables:

$$\begin{cases} u = x - \bar{x}_i \\ v = y - \bar{y}_i, \end{cases} \quad (28)$$

where  $i = 1, 2$ , depending on the point we are interested in. Thus, our system (7) can be recast as

$$\begin{pmatrix} \dot{u} \\ \dot{v} \end{pmatrix} = \begin{pmatrix} 0 & -\Omega \\ \Omega & 0 \end{pmatrix} \begin{pmatrix} u \\ v \end{pmatrix} + \begin{pmatrix} F(u, v) \\ G(u, v) \end{pmatrix}, \quad (29)$$

where

$$F(u, v) = \left( -1 + \alpha \sqrt{(u + \bar{x}_i)^2 + (v + \bar{y}_i)^2} - ((u + \bar{x}_i)^2 + (v + \bar{y}_i)^2) \right) (u + \bar{x}_i) - \Omega \bar{y}_i + I$$

$$G(u, v) = \left( -1 + \alpha \sqrt{(u + \bar{x}_i)^2 + (v + \bar{y}_i)^2} - ((u + \bar{x}_i)^2 + (v + \bar{y}_i)^2) \right) (v + \bar{y}_i) + \Omega \bar{x}_i.$$

It is easy to check that the functions  $F(u, v)$  and  $G(u, v)$  satisfy the conditions above. Furthermore, evaluating their partial derivatives, it is possible to observe that  $G_u = F_v$ , which implies  $G_{uu} = F_{uv}$ ,  $G_{uv} = F_{vv}$ , and  $G_{uuv} = F_{uvv}$ . Expression (27) reduces to

$$a = \frac{1}{16} (F_{uuu} + 2F_{uvv} + G_{vvv}). \quad (30)$$

Computing these partial derivatives and evaluating them in  $(0, 0)$ , we get

$$a = \frac{1}{16} \left( -16 + \frac{3\alpha}{\sqrt{\bar{x}_i^2 + \bar{y}_i^2}} \right). \quad (31)$$

Recalling that from (11) we have  $\bar{x}_i^2 + \bar{y}_i^2 = \frac{I}{\Omega} \bar{y}_i = \bar{\zeta}_i^2$ , we obtain

$$a = \frac{1}{16} \left( -16 + \frac{3\alpha}{\bar{\zeta}_i} \right) \quad (32)$$

and therefore

$$a|_{P_1} = \frac{1}{16} \left( -16 + \frac{3\alpha}{\zeta_1} \right) = -1 + \frac{3\alpha}{2(3\alpha - \sqrt{9\alpha^2 - 32})} > 0. \quad (33)$$

Therefore, we conclude that for every  $\alpha > 2$  and  $\Omega > \frac{5}{16}$ , in  $P_1$  we have a subcritical Hopf bifurcation. Analogously, evaluating the quantity  $a$  in  $P_2$  we obtain:

$$a|_{P_2} = \frac{1}{16} \left( -16 + \frac{3\alpha}{\zeta_2} \right) = -1 + \frac{3\alpha}{2(3\alpha + \sqrt{9\alpha^2 - 32})} < 0. \quad (34)$$

In this case we expect a supercritical Hopf bifurcation for every  $\alpha > 2$  and  $\Omega > 1$ . Both the results have been confirmed by time-domain numerical simulations (see also Figure 3).

We now turn our attention to saddle-node bifurcations of equilibria, that are characterized by  $\det J = 0$ , since they involve the presence of a null eigenvalue (Kuznetsov, 2004). Using (18) we obtain

$$I^2 = -2\bar{\zeta}^6 + 3\alpha\bar{\zeta}^5 - (2 + \alpha^2)\bar{\zeta}^4 + \alpha\bar{\zeta}^3. \quad (35)$$

Because the Jacobian is evaluated in the equilibrium configurations, we recall that  $\bar{\zeta}$  will be a root of (13). Thus, substituting (35) in (13) we obtain

$$\bar{\zeta}^2 \left[ 3\bar{\zeta}^4 - 5\alpha\bar{\zeta}^3 + 2(2 + \alpha^2)\bar{\zeta}^2 - 3\alpha\bar{\zeta} + (1 + \Omega^2) \right] = 0. \quad (36)$$

We conclude that, for any fixed value of the parameter  $\Omega$ , we have a saddle-node bifurcation at the equilibrium points that satisfy:

$$3\bar{\zeta}^4 - 5\alpha\bar{\zeta}^3 + 2(2 + \alpha^2)\bar{\zeta}^2 - 3\alpha\bar{\zeta} + (1 + \Omega^2) = 0$$

for the values of  $I$  given by (35).

**Remark 2.** *The conditions for the occurrence of a saddle-node bifurcation leads to the same set of curves in the  $\Omega - I$  plane of Figure 4. This is due to the fact that a zero eigenvalue for the Jacobian matrix of a generic dynamical system  $\dot{x} = f(x)$  implies that the equilibrium point has a multiplicity equal to two as zero of the function  $f(x)=0$  (Kuznetsov, 2004).*

Finally, we consider the case

$$\begin{cases} \text{tr} J = 0 \\ \det J = 0 \end{cases} \quad (37)$$

that corresponds to a codimension 2 bifurcation, the so-called Bogdanov-Takens one. In our case, we have previously seen that the trace of the Jacobian matrix is equal to zero at the points  $P_1$  and  $P_2$ , with  $I_i$  given by (22). The further condition on the determinant of  $J$  leads to the following critical values of  $\Omega$ :

$$\begin{aligned} P_1 &\Rightarrow \Omega_1^2 = \frac{9}{512}\alpha^4 + \frac{1}{4} - \frac{1}{8}\alpha^2 + \left( \frac{3}{512}\alpha^3 - \frac{1}{32}\alpha \right) \sqrt{9\alpha^2 - 32} \\ P_2 &\Rightarrow \Omega_2^2 = \frac{9}{512}\alpha^4 + \frac{1}{4} - \frac{1}{8}\alpha^2 + \left( -\frac{3}{512}\alpha^3 + \frac{1}{32}\alpha \right) \sqrt{9\alpha^2 - 32}. \end{aligned} \quad (38)$$

In particular for  $\alpha = 3$  we have

$$P_1 = \left( -\frac{5}{16\Omega}, \frac{\Omega}{16I_1} \right) \quad \text{with} \quad I_1 = \frac{\sqrt{25 + 256\Omega^2}}{8}$$

$$P_2 = \left( -\frac{1}{\Omega}, \frac{4\Omega}{I_2} \right) \quad \text{with} \quad I_2 = 2\sqrt{1 + \Omega^2}$$

and, exploiting (38), we conclude that in

$$(\Omega, I) = \left( \frac{5}{16}, \frac{5}{64}\sqrt{2} \right) \quad \text{and} \quad (\Omega, I) = (1, 2\sqrt{2})$$

we have two Bogdanov-Takens bifurcations.

### 3.2. Global bifurcations

Time-domain numerical simulations reveal that, for some couple  $(\Omega, I)$  shown in Figure 4, the saddle-node bifurcations of equilibria are nontrivial, in the sense that they involve the appearance and disappearance of limit cycles.

Firstly introduced and studied in (Andronov et al., 1973), in system (7) it involves the disappearance of the periodic solutions. In literature, this bifurcation goes by several names: saddle-node on limit cycle (SNLC) (Hoppensteadt & Izhikevich, 1997), saddle-node on invariant cycle (SNIC) (Izhikevich, 2006), saddle-node infinite period (SNIPER) (McCormick et al., 1991) or saddle-node homoclinic bifurcation (Kuznetsov, 2004). In particular, its name saddle-node on invariant cycle is due to the fact that it is a standard saddle-node, but occurs on an invariant cycle (Izhikevich, 2006). Let us suppose that the system exhibits a periodic solution, as in Figure 6 (a). The emergence of a saddle-node (see Figure 6 (b)) coincides with the break of the limit cycle, that becomes a homoclinic trajectory. As the bifurcation parameter increases (see Figure 6 (c)), the node and the saddle move away each other and two heteroclinic trajectories arise to connect the two equilibria.

It is worth remarking that this bifurcation is both global and local, as it involves a simultaneous collision of equilibria and manifolds (Kuznetsov, 2004). In fact, as we have shown in the previous section, local analysis describes only the saddle-node bifurcation of equilibria, missing the disappearance of the limit cycle.

In general, detecting a homoclinic trajectory is not a simple task. A possible evidence of a SNLC bifurcation is given by the period of the limit cycle. In fact, the closer is the parameter to the critical value, the larger is the period of the corresponding limit cycle, that tends to infinity approaching the SNLC bifurcation.



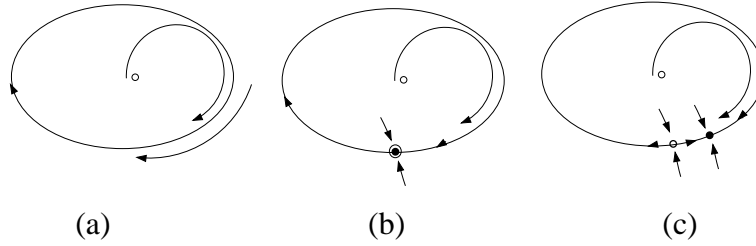


Figure 6: Saddle-node bifurcation on limit cycle (SNLC).

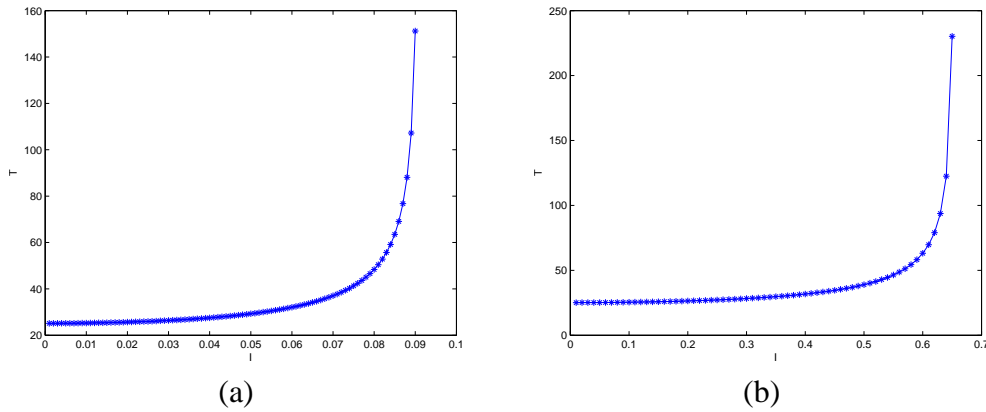


Figure 7: Period  $T$  of the unstable (a) and stable (b) limit cycles as function of the external input  $I$ , for  $\Omega = 0.25$ . In  $I_{c1} = 0.091$  and  $I_{c2} = 0.653$  the system undergoes two SNLC bifurcations, that entail the disappearance in succession of the two limit cycles.

Furthermore, the system spends more time near the place where the saddle-node will appear, in a sort of sense having a hunch of the future bifurcation.

As an example, let us consider the case  $\Omega = 0.25$ , for which it is possible to see that our system undergoes two SNLC bifurcations. In Figure 7 the periods of the two (stable and unstable) limit cycles as function of the external input are shown. It is worth observing that the two periods tend to infinity, approaching the bifurcation points  $I_{c1} = 0.091$  and  $I_{c2} = 0.654$  (see also Figures 3(a-b)), respectively.

In Figure 8 the wave forms for the  $x$ -component of the two limit cycles in proximity of the respective SNLC bifurcations are represented. Notice the analogy with dynamics of the so-called relaxation oscillators.

It is possible to see that the system tends to stay for the majority of the time around one configuration, that is precisely where the saddle-node appears at the bifurcation point. In order to characterize the positions in the phase plane where

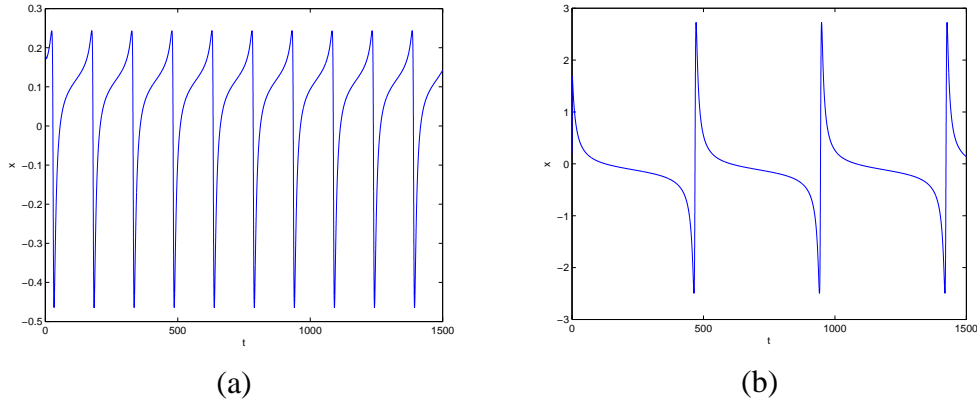


Figure 8: Wave form of the unstable (a) and stable (b) limit cycles ( $x$ -component), in proximity of SNLC bifurcations ( $I = 0.090$  and  $I = 0.654$ , respectively). The frequency  $\Omega$  is set equal to 1.

the system spends most of the time, a histogram of the dynamics arising from the simulations in the time-domain ( $t_{fin} = 1500$  and  $\Delta t = 0.01$ ) has been computed (see Figure 9). Since for  $I_{c1} = 0.091$  the saddle-node has coordinates  $SN1 = (0.1081, 0.3284)$ , while for  $I_{c2} = 0.654$  we have  $SN2 = (-0.1368, 2.6066)$ , the check with Figure 9 leads to the expected conclusions. The same approach has been carried out for both the two limit cycles in absence of external input ( $I = 0$ ), to make a comparison with the previous relaxation oscillator-like behavior. In this case, basically all the states are uniformly visited by the system. The two peaks at minimum and maximum values are due to the discretization of the variables for the histogram computation.

It is worth observing that, in order to obtain Figures 7, 8 and 9 for the unstable limit cycle, the numerical simulations have been performed back in time.

#### 4. Conclusion

Cyclic Negative Feedback Systems (CNF systems) are one of the most exploited mathematical frameworks to model phenomena arising in systems biology, such as cascades of molecular reactions inside the cell. Since it is well known that these events take place in different compartments, it seems more appropriate to consider networks of diffusively coupled CNF systems. In addition, the effect of an external agent, such as the light, the temperature or the synthesis of the substrate, is suitably modeled as a constant external term. Unfortunately, due to the huge number of factors involved in such mechanisms, networks of coupled CNFs

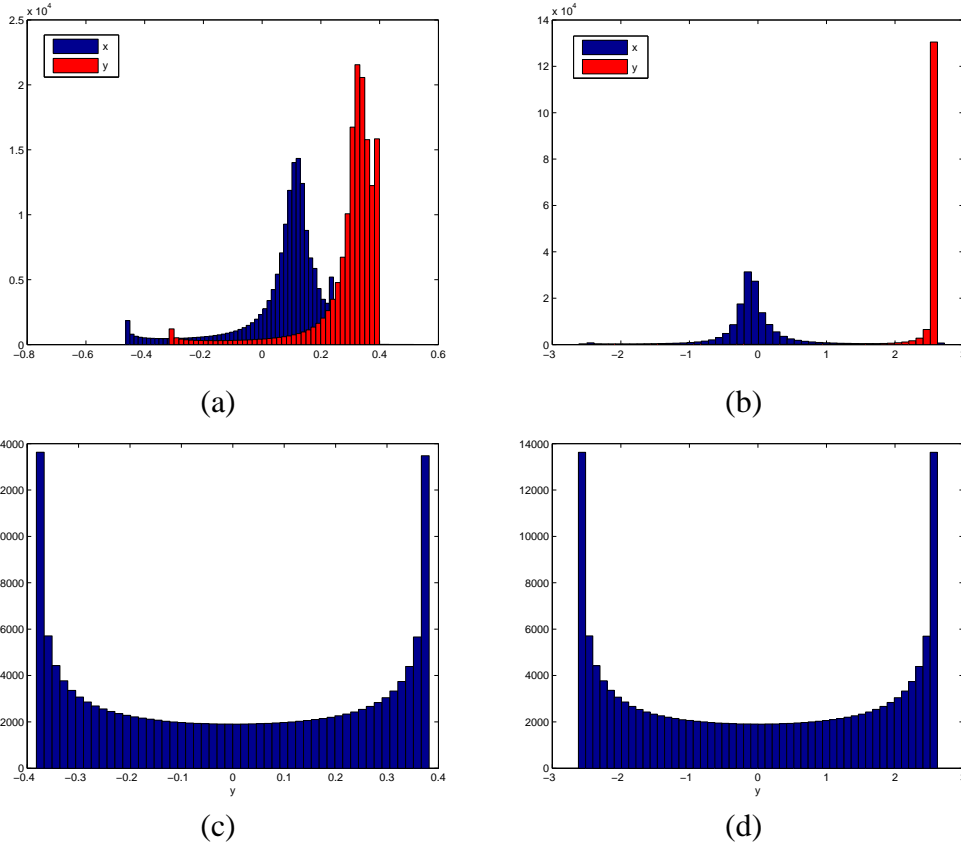


Figure 9: Histogram of the unstable (a-c) and stable (b-d) limit cycle dynamics near the SNLC bifurcation ( $I = 0.090$  and  $I = 0.653$  in (a) and (b), respectively) and far away from the critical values of the bifurcation parameter ( $I = 0$  in both (c) and (d)).

systems can be high-dimensional, and therefore their dynamics can be difficult to fully characterize.

Inspired by the complex spatio-temporal patterns found in arrays of diffusively coupled Cyclic Negative Feedback systems (CNF systems), we have considered the case of radial isochron clocks that exhibit the coexistence of different stable attractors, as well as CNF systems. In fact, these systems present the same qualitative behavior of CNF systems, but they are quite easy to handle since they are of lower order. In particular, we have dealt with systems that present a hard excitation behavior, i.e., that display at the same time a stable equilibrium point and a stable limit cycle.

As a first step, we have focused on the effect of a constant external input on

a single radial isochron clock with hard excitation. We have carried out a characterization of local and global bifurcations, and in particular, we have detected the occurrence of saddle-node on limit cycle bifurcations. It is interesting to notice that, in presence of such bifurcations, the system exhibits a relaxation oscillator-like dynamics.

Once we have completely analyzed the dynamical behavior of a single system in presence of a constant external input, we are now interested in considering networks of diffusively coupled radial isochron clocks, in order to investigate the complex dynamics that may arise due to the additional effect of coupling.

### **Acknowledgment**

This work was partially supported by the CRT Foundation. L. Ponta acknowledges the Istituto Superiore Mario Boella for financial support. V. Lanza and M. Bonnin acknowledge the Istituto Superiore Mario Boella and the regional government of Piedmont for financial support.

### **References**

- Andronov, A., Leontovich, E., Gordon, I., & Maier, A. (1973). *Theory of Bifurcations of Dynamical Systems on a Plane*. Wiley, New York.
- Arcak, M., & Sontag, E. (2008). A passivity-based stability criterion for a class of interconnected systems and applications to biochemical reaction networks. *Mathematical Biosciences and Engineering*, 5, 1–19.
- Bastin, G., & Dochain, D. (1990). *On-line estimation and adaptive control of bioreactors*. Elsevier.
- Boushel, C., & Curran, P. (2007). The bifurcation behaviour of a novel second order model of the Hodgkin-Huxley neuron. In *Proceedings of ECCTD* (pp. 1034–1037).
- Cohen, H. (1993). *A Course in Computational Algebraic Number Theory*. Springer New York.
- Elowitz, M., & Leibler, S. (2000). A synthetic oscillatory network of transcriptional regulators. *Nature*, 403, 335–338.

- Goldbeter, A., & Berridge, M. (1997). *Biochemical oscillations and cellular rhythms: The molecular bases of periodic and chaotic behaviour*. Cambridge Univ Press.
- Goldbeter, A., Gonze, D., Houart, G., Leloup, J., Halloy, J., & Dupont, G. (2001). From simple to complex oscillatory behavior in metabolic and genetic control networks. *Chaos*, *11*, 247–260.
- Guckenheimer, J., & Holmes, P. (1983). *Nonlinear Oscillations, Dynamical Systems, and Bifurcations of Vector Fields*. New York: Springer-Verlag.
- Hoppensteadt, F. C., & Izhikevich, E. M. (1997). *Weakly Connected Neural Networks*. New York: Springer-Verlag.
- Izhikevich, E. (2001). Synchronization of elliptic bursters. *SIAM Review*, (pp. 315–344).
- Izhikevich, E. (2006). *Dynamical systems in neuroscience: The geometry of excitability and bursting*. The MIT press.
- de Jong, H. (2002). Modeling and simulation of genetic regulatory systems: a literature review. *Journal of Computational Biology*, *9*, 67–103.
- Jovanic, M., Arcak, M., & Sontag, E. (2008). A passivity-based approach to stability of spatially distributed systems with a cyclic interconnection structure. *Automatic Control, IEEE Transactions on*, *53*, 75–86.
- Kholodenko, B. (2000). Negative feedback and ultrasensitivity can bring about oscillations in the mitogen-activated protein kinase cascades. *Eur. J. Biochem*, *267*, 1583–1588.
- Kuznetsov, Y. A. (2004). *Elements of Applied Bifurcation Theory*. New York: Springer-Verlag.
- Lanza, V., Corinto, F., & Gilli, M. (2009). Diffusive coupled cyclic negative feedback systems. In *Proceedings of IJCNN, IEEE International Joint Conference on Neural Networks* (pp. 1714–1721).
- Leloup, J., & Goldbeter, A. (2001). A molecular explanation for the long-term suppression of circadian rhythms by a single light pulse. *Am. J. Physiol. Regulatory Integrative Comp. Physiol.*, *280*, 1206–1212.

- Liu, J. (2002). State selection in coupled identical biochemical systems with co-existing stable states. *BioSystems*, 65, 49–60.
- Mallet-Paret, J., & Smith, H. (1990). The Poincaré-Bendixson theorem for monotone cyclic feedback systems. *Journal of Dynamics and Differential Equations*, 2, 367–421.
- McCormick, W., Noszticzius, Z., & Swinney, H. (1991). Interrupted separatrix excitability in a chemical system. *J. Chem. Phys.*, 94, 2159.
- Minorsky, N. (1974). *Nonlinear Oscillations*. Huntington, New York: Krieger.
- de Paor, A. M. (1994). Liapunov, Poincaré-Bendixson and cardiac fibrillation. *Lek. a Technika*, 4, 75–79.
- Thron, C. (1991). The secant condition for instability in biochemical feedback control - I. The role of cooperativity and saturability. *Bulletin of Mathematical Biology*, 53, 383–401.
- Tyson, J., & Othmer, H. (1978). The dynamics of feedback control circuits in biochemical pathways. *Progress in Theoretical Biology*, 5, 1–62.
- Winfree, A. T. (2001). *The geometry of biological time*. Springer Verlag.